Electrochemistry of Conductive Polymers. 30. Nanoscale Measurements of Doping Distributions and Current−Voltage Characteristics of Electrochemically Deposited Polypyrrole Films

Hyo Joong Lee and Su-Moon Park*

Department of Chemistry and Center for Integrated Molecular Systems, Pohang University of Science and Technology, Pohang, Gyeongbuk 790-784, Korea (Republic of Korea)

Received: June 22, 2003; In Final Form: November 26, 2003

Spatial variations in electronic structures and evolutions of band structures of polypyrrole (PPy) have been studied using an atomic force microscope with a conducting tip, a so-called current-sensing atomic force microscope (CS-AFM). PPy films were deposited electrochemically onto gold-on-silicon electrodes, and their doping levels were controlled by successive electrochemical reduction. The topographic and current images of PPy surfaces were obtained simultaneously with nanometer scale spatial resolution using the CS-AFM. Galvanostatically prepared PPy films showed almost uniform current images even when the bias voltage was reduced to as small as 3 mV. High current flowing regions gradually disappeared starting from the top of the globules as the film was reduced progressively, indicating the top of the globules is preferentially reduced. The supporting electrolytes and solvents used during electrochemical preparation of PPy films also affected the doping distribution; the doping can be either nearly uniform or islandlike. The point-contact current−voltage ($I-V$) characteristics of conducting tip−polymer−Au substrate systems were investigated as a function of the degree of doping, and various $I-V$ curves representing metallic, semiconducting, and insulating states were obtained depending on the doping level of the film.

Introduction

In recent years, nanoscale electronic devices using organic materials such as single molecules,[1] supramolecules,[2] carbon nanotubes,[3] self-assembled monolayers,[4] and (conducting) polymers[5] have attracted much attention for the construction of fast, inexpensive, and dimensionally ultimate devices as a bottom-up approach.[6] Based on these materials, many kinds of molecular electronic devices have been constructed and their electrical properties measured and evaluated by various methods.[7] As has been found in the literature, it is very difficult but important to reproducibly and accurately measure and evaluate the electrical properties of the candidate materials for molecular electronic devices.[8] Until now, scanning tunneling microscopy (STM) has been widely used to measure the electrical characteristics of single molecules and their assemblies that are of interest to molecular electronics.[9] However, use of the STM technique for this purpose is limited to conducting materials or very thin nonconducting materials due to typical tunneling distances (1−10 nm). The STM results also include the vacuum gap between the tip and molecules probed, which can cause complexity and ambiguity in the interpretation of intrinsic properties of molecules.

Competing or complementary with STM, atomic force microscopy with a conducting tip (CS-AFM) has found its applications in many areas during the past decade because it allows an easy contact to be made with various substances including organic materials.[10] Topographical and current images could be obtained simultaneously for various systems, which provide otherwise impossible information on the distribution of conducting islands surrounded by insulating areas and relations between structural features and electrical properties on the nanometer scale.[11] By measuring the current−voltage ($I-V$) traces, electronic transports through single molecules,[12] self-assembled monolayers,[13] carbon nanotubes,[14] quantum dots,[15] and others[16] have been widely investigated. The reproducible new results obtained by this technique describe the advantages of this method.

Conducting polymers are straightforwardly prepared by chemical or electrochemical methods,[17] and their electronic states can be reversibly changed between insulating and conducting states by electrochemical redox reactions. The polymers have been used in a variety of systems such as chemical sensors, energy conversion devices, corrosion protection layers, electrochromic devices, and electronic circuits.[17] In all these applications, their bulk or interfacial electrical properties are used and sometimes these properties need to be controlled for specific purposes. Therefore, the dopant ion distribution in the matrix of conducting polymers and electron transfer through the interface are key factors in determining performances of devices made of conducting polymers. Until now, however, only macroscopic or average characteristics such as conductivities, band gaps, and redox potentials have been measured. In addition, it would be very important to have a good understanding of their interfacial electronic states, their electron transport properties, and how homogeneous they are, if one wants to take advantage of their electrical properties in nanoscale devices.

There have been a few reports on the electronic states of conducting polymer films studied using STM and Kelvin probe methods. The STM technique is usually limited to very thin films or conducting states,[18] and the Kelvin probe method can be used only for mapping the surface potential, not for direct quantitative studies.[19] A decided advantage of the AFM technique is that the contact can be made between the conduct-

* Corresponding author. Telephone: +82-54-279-2102. Fax: +82-54-279-3399. E-mail: smpark@postech.edu.

10.1021/jp035766a CCC: $27.50
Published on Web 01/06/2004

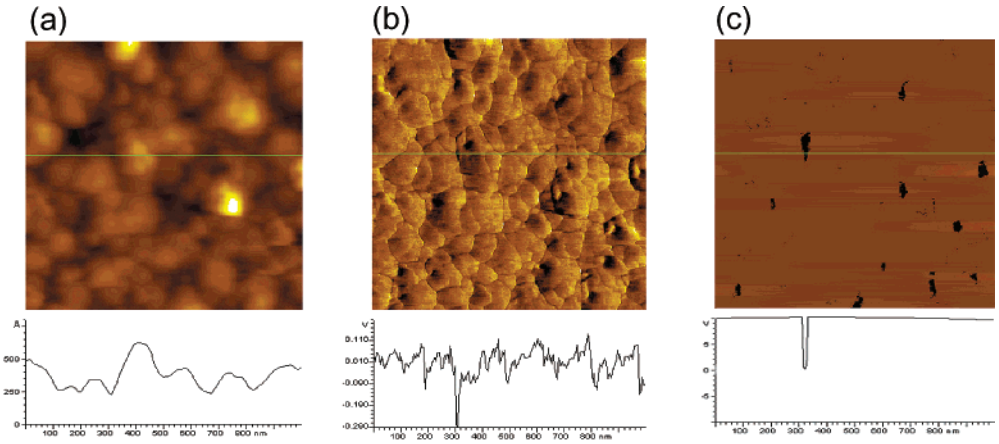

Figure 1. Concurrently obtained AFM images of typical topography (a), friction (b), and current (c) for an as-grown PPy film in a 0.10 M $LiClO_4$ acetonitrile solution containing 2.0% water and their cross-sectional analyses. The scan area was 1 × 1 μm. In the current image (c), the full-scale current was 100 nA; the current conversion factor was 10 nA/V.

ing tip and the substrate with a certain confidence by maintaining a prescribed load force. In this paper, we demonstrate that the current-sensing AFM could be applied to reveal both the spatial doping distribution by mapping current images and the band gap by measuring $I-V$ curves as a function of the doping level of the polypyrrole (PPy) films.

Experimental Method

Acetonitrile (ACN, Aldrich, 99.8%, anhydrous) was used as received. Lithium perchlorate ($LiClO_4$, Aldrich, 99.99%), lithium tetrafluoroborate ($LiBF_4$, Aldrich, 98%), and tetraethylammonium tetrafluoroborate ($TEABF_4$, Aldrich, 99%) were used after drying in a vacuum oven at 110 °C for 16 h. Pyrrole (Aldrich, 98%) was used after distillation over zinc powder and stored in the dark under a nitrogen atmosphere. An electrochemical cell with a three-electrode configuration was used for electrochemical experiments. Gold on silicon (with Cr adhesive layers, LGA films) was annealed by a hydrogen flame and used as a working electrode (diameter 5.7 mm). Platinum gauze and a silver wire dipped in a 0.10 M $AgNO_3$ solution in ACN in a separate compartment were used as counter and reference electrodes, respectively. In aqueous media, an Ag/AgCl (in saturated KCl) electrode was used as a reference electrode instead. PPy films were grown galvanostatically by applying 1.0 mA (=3.92 mA/cm^2) for 10 s after purging with N_2 for 1 h through an acetonitrile solution containing 2% water, 0.10 M pyrrole, and 0.10 M $LiClO_4$ ($LiBF_4$ or $TEABF_4$) using an EG&G Model 273 potentiostat−galvanostat.[20] As-formed PPy films were in oxidized states, which were reduced successively by stepping the potential to −0.50 V for a given length of time in a monomer-free electrolyte solution. After electrochemical synthesis, the films were rinsed with pure ACN and dried under vacuum at room temperature. The film thickness was determined to be about 110 nm by a Veeco Instruments Dektak3 surface profiler, which agrees well with a reported value assuming that 379 mC corresponds approximately to 1.0 μm.[21]

The contact mode AFM with a current-sensing module, so-called current sensing AFM (PicoSPM, Molecular Imaging Inc.),[22] was used to simultaneously obtain topographical and current images. This modification did not deteriorate the spatial resolution of the AFM significantly, which was shown to be about 2 nm in our experiment when a narrower region was scanned (not shown); similar results have been reported in the literature for AFM measurements with a conducting tip.[12d,13e] The gold-coated Si_3N_4 cantilevers (spring constant 0.12 N/m) were purchased from Olympus Co. The load force was maintained at 3−5 nN to avoid damage to the tip and the sample. A bias voltage between the substrate (Au) and conducting cantilever (which is grounded) was 50 mV during all the imaging experiments. Before imaging of the PPy surfaces, the surface was purged by high purity N_2 gas to minimize the effects of moisture, and all the AFM experiments were carried out under this controlled environment. The topographical and current images recorded before, during, and after the point-contact $I-V$ measurements were identical as long as the load force was maintained between 3 and 5 nN, indicating that the tips were not damaged during the measurements. The data were discarded whenever the images were different before, during, or after a series of electrical measurements.

Results and Discussion

Figure 1 shows typical topography (a), friction (b), and current (c) images obtained simultaneously for an identical part of the surface of a PPy film galvanostatically grown in acetonitrile containing 0.10 M $LiClO_4$. The globular-shaped structure in the topographical image is typical for thickness below 1 μm, although the size and shape are slightly different depending on the growth conditions.[20,23] The friction image provides a clearer picture of globular structures, which is not the case in the topographic image due to its lower contrast, but it reflects only the morphology, not the current distribution, of the film. The current map shows that the current flows rather uniformly over the entire surface area through the PPy film from the substrate to the tip except for some small areas (black spots) at the current sensitivity used for our measurements, i.e., 100 nA, which is the maximum value our current amplifier can handle. Currents higher than 100 nA were recorded throughout almost the whole film surface except for some spots. The currents higher than 100 nA were measured at the fully doped (oxidized) PPy films prepared by the galvanostatic method even at a bias potential of as small as 3 mV.

Since the current went over the saturation level, we could not distinguish the degree of doping levels between various points on the surface as can be seen in Figure 1. We thus reduced the PPy film to see the differences in the doping states at various locations on the surface. First, we stepped the potential to −0.50 V and reduced the film for 30 s in acetonitrile containing only the supporting electrolyte. Then, the PPy film was dried and examined under the same experimental conditions as those used for Figure 1. The topography image shown in Figure 2a is

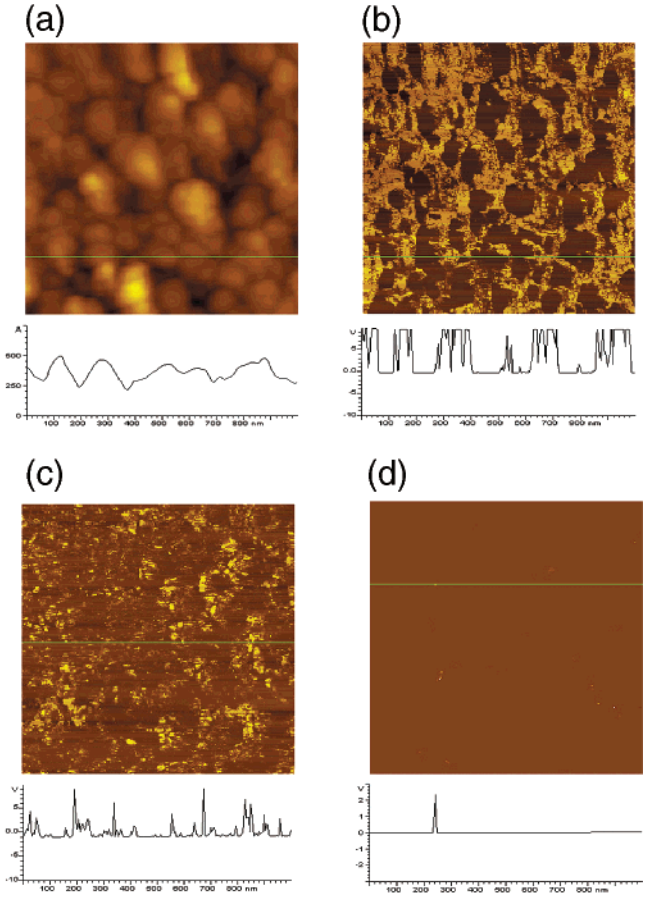

Figure 2. Topographic (a) and current images simultaneously recorded for the same PPy film surface as used for Figure 1 after reducing it at −0.50 V successively for 30 s (b), an additional 3 min (c), and an additional 5 min (d) in a 0.1 M $LiClO_4$ ACN solution containing no water and pyrrole monomers.

practically identical to that in Figure 1a after the dedoping process, but the current image shown in Figure 2b has been changed rather drastically such that there are regions where almost no current flows at the same bias potential (50 mV), which may be compared with the image shown in Figure 1c. As can be seen, the doped (high current flowing) and dedoped (no current flowing) regions are clearly distinguished, with the dedoping process not taking place homogeneously over the entire area. It is seen fairly clearly from the comparison of Figure 2a and Figure 2b that the top region of globules is reduced preferentially where no currents are seen to flow. This is perhaps due to the fact that the top region is more oxidized and, thus, more conductive, which is in general agreement with the results obtained from the Kelvin probe method.[19] When a spot is more oxidized, it may accept electrons more easily than the other locations due to a larger conductivity at the spot. When the same film was subjected to electrochemical reduction for an additional 3 min (Figure 2c), the regions where no currents flow were spread over the surface and the magnitudes of currents were reduced to a great extent. Most of the boundary regions have been reduced at this dedoping stage. When the film was reduced for another 5 min, almost no current flows over the entire area except for a few spots (Figure 2d) where the current is very small as can be seen from the cross-sectional analysis shown below the current image.

The results described here indicate that the fully doped and fully dedoped PPy films show rather homogeneous electrical characteristics within the sensitivity of the instrument currently available for the measurements, while partially doped films are fairly inhomogeneous. When an instrument of a higher current scale is available, however, the fully doped film may turn out to be inhomogeneous.

Since we have examined the effects of electrochemical reduction of the PPy film prepared in acetonitrile, we now describe our study on the effects of electrolytes and the solvent on the conductivity of the PPy film. When the supporting electrolyte was changed from ClO_4^- to BF_4^- and the film was prepared under otherwise identical experimental conditions, the current images were dramatically different from those shown in Figures 1c and 2, although the topographical images (not shown) were about the same as those shown in Figures 1a and 2a. Figure 3a shows that the change in anions of the supporting electrolyte led to an inhomogeneous current image instead of the uniform pattern shown in Figure 1c. One can see from Figure 3a that the islands, at which high currents flow, are isolated by large insulating regions. Further, the conductive islands did not necessarily correspond to the top of the globules (not shown). Effects of the cation of the supporting electrolyte for the same anion BF_4^-, i.e., Li^+ vs TEA^+ (tetraethylammonium ion), were also very similar except that the sizes of islands are larger in the case of TEA^+ in Figure 3b. When the solvent was changed to an aqueous medium, the current image was significantly different from those obtained in nonaqueous media as can be seen in Figure 3c, but the topographical image was similar to that of the film prepared in acetonitrile although the details of globules were not the same. The high current flowing regions are fairly homogeneously dispersed and the currents are significantly lower than the limiting value, which should be compared to those found in the film prepared in acetonitrile. These observations are attributed to the hydrophilic nature of the ═N−H group of pyrrole molecules and the reaction products produced by overoxidation of PPy during electrochemical polymerization of pyrrole,[24] which introduces the surface oxides responsible for low or nonconductive areas relatively homogeneously dispersed throughout the film. The different current patterns and magnitudes shown here depending on experimental conditions would explain different conductivities and electrical properties reported for the bulk conducting polymer films prepared under different experimental conditions; it is well-known that conductivities of PPy films depend strongly on the nature of the anions and solvents used in the polymerization process.[25−28] Our observation is in good agreement with the bulk conductivities of the PPy films prepared in different media with different supporting electrolytes.[25] It shows that the films prepared in acetonitrile containing 2% water with $LiClO_4$ used as a supporting electrolyte show the best performance with the homogeneity and highest conductivity.

In efforts to assess the conductivities of these films more quantitatively depending on the doping levels, we obtained the current−voltage ($I-V$) curves at some selected spots. The results are shown in Figure 4A. Here, the line shown as Figure 4A(a), which looks much like a vertical line, presents the $I-V$ curve of the as-prepared film over 10 mC (Figure 1c). Line b was taken from a more conducting spot of the film reduced at −0.50 V for 30 s over about 700 μC (Figure 2b). Traces c and d were obtained from less conducting spots (dark and darker areas) of the same scanned area. Curve e was taken from a less conducting area of the film shown in Figure 2c, which had been reduced for an additional 3 min at −0.50 V over 1180 μC. Line f was obtained from a nonconducting spot in the dark area of the film shown in Figure 2d, which was reduced for an additional 5 min at −0.50 V using 1630 μC, and it can be seen that the film is

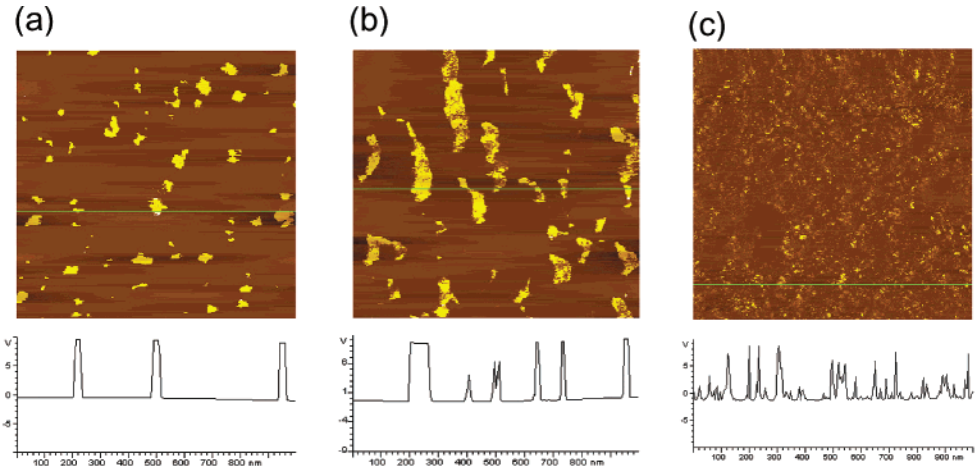

Figure 3. Typical 1 × 1 μm current images and their cross-sectional analyses. The scanned PPy films were prepared in ACN containing 2% H_2O as well as 0.10 M $LiBF_4$ (a) and $TEABF_4$ (b), respectively. (c) The film was prepared in an aqueous medium containing 0.10 M $TEABF_4$ under otherwise identical conditions.

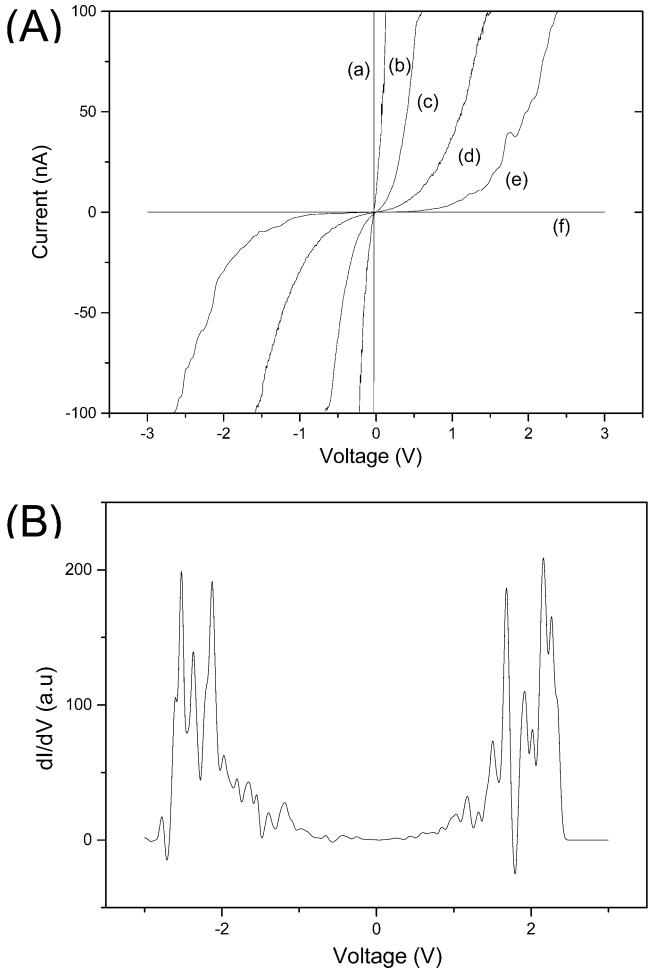

Figure 4. (A) Current−voltage curves obtained from (a) a randomly picked spot in the film shown in Figure 1c, (b)−(d) randomly picked spots from the film shown in Figure 2b, (e) a spot in the film shown in Figure 2c, and (f) a spot in Figure 2d. Each curve shows an average of over 10 signals. (B) The dI/dV signal of curve e in (A).

almost perfectly insulating with the line almost horizontal. Our results show that various $I-V$ curves can be obtained when the point-contact measurements are made over partially reduced surfaces such as that shown in Figure 2b,c. Ohmic $I-V$ curves identical with that shown as trace a were obtained reproducibly throughout the large doped surface (Figure 1c). The $I-V$ traces move from ohmic (trace a) to semiconductor-like characteristics such as traces b through e depending on which spots the data were taken from on the same film as shown in Figure 4A. These curves represent the typical $I-V$ traces obtained frequently and reproducibly depending on doping states of the films. Perhaps all the $I-V$ curves display exponential increases until they saturate at the highest full-scale current of 100 nA. It appears that traces a and b show simply the early linear parts of the increases, which make them look ohmic. Whether or not curves a−d are simply earlier parts of a curve like trace e with the saturated part not shown needs to be studied further. That is, it would be interesting to see how the traces would increase with increases in applied voltage if the full-scale current of our instrument were much higher than the one used in this study, i.e., 100 nA. One has to use an instrument with much larger current capability, for example, 1 mA full scale.

To obtain the band gap of a semiconductive PPy film, the dI/dV signal was taken from the $I-V$ curve shown in trace e because it has a relatively wide potential range before it gets to the saturation point, and the result is shown in Figure 4B. Similar measurements have been reported for conducting polymers[18a,d,e] and for carbon nanotubes.[18f] The $I-V$ curves shown in Figure 4A, as well as the dI/dV signal in Figure 4B, are rather symmetrical with respect to 0 V, indicating that the signals are not the same as those observed from typical semiconductor−metal junctions. A typical semiconductor−metal junction shows different current responses for forward and reverse biases,[29] which is not the case here. Thus, the PPy film examined here does not show typical $I-V$ characteristics of a true semiconductor. Instead, the PPy film shows a behavior of a heavily doped semiconductor with many states present within the band gap.

As can be seen, the band gap may be estimated to be between about 2.3 and 3.8 eV, depending on which peak signals are taken for band gap estimation from various band edges shown as peaks in the derivative signals (Figure 4B). The band gaps are estimated from the distances between the dI/dV peaks.[18f] There are a number of band edges, probably because various states generated during the doping process are located within the band gap due to the introduction of polarons and bipolarons, which also widens the band gap. The band gap widening is well-known for conducting polymers upon electrochemical doping.[30] The band gap of PPy is estimated to be 3.2 eV from the band gap transition of 387 nm when it is fully dedoped where no other states would be present within the band gap. The semiconductor properties derived from conducting polymers could be different

from those of true semiconductors. Conducting polymers become metal-like conductors when heavily doped because interstate bands arising from bipolarons make the band gap small enough to make the holes move around rather freely upon applying a bias voltage. Depending on the doping level, not only the band gaps but also the population of the dopants would be different, leading to different conductivities. It is for this reason that various I/V curves can give various band gaps as can be seen from $I-V$ curves shown in Figure 4A.

Conclusion

In conclusion, we have demonstrated that the CS-AFM is an excellent tool for monitoring the changes of spatial doping distribution and current−voltage characteristics as a function of the doping level of conducting polymers by measuring the current flowing through Au-coated tip/polymer/Au substrates. The PPy film has been studied as an example, which can be described to be rather uniform in terms of its electrical properties within the current handling capabilities of our instrument when it is fully doped in contrast to earlier reports, in which conducting polymer films are inhomogeneous in their electrical properties.[31] The highly doped (high current flowing) regions of the PPy film disappeared gradually upon electrochemical reduction by dedoping first at the top of globules, followed by successive dedoping in the boundary region and leading at last to the fully dedoped state. The $I-V$ traces also moved from an ohmic behavior, through various semiconducting characteristics, and eventually to an insulating state as the dedoping process was progressed.

We conclude that the technique is useful in studying relations between electrical properties and preparation conditions of conducting polymers and also finding optimum conditions for specific purposes. Also, the electrical behavior of the PPy−gold junction is found to be different from that of a typical semiconductor−metal junction.

Acknowledgment. This work was supported by the National R&D Project for Nano Science and Technology of the Ministry of Science and Technology of Korea.

References and Notes

(1) (a) Aviram, A. *Chem. Phys. Lett.* **1974**, *29*, 277. (b) Park, J.; Pasupathy, A. N.; Goldsmith, J. I.; Chang, C.; Yaish, Y.; Petta, J. R.; Rinkoski, M.; Sethna, J. P.; Abruna, H. D.; Mceuen, P. L.; Ralph, D. C. *Nature* **2002**, *417*, 722. (c) Park, H.; Park, J.; Lim. A. K. L.; Anderson, E. H.; Alivisatos, A. P.; Mceuen, P. L. *Nature* **2000**, *407*, 57. (d) Liang, W.; Shores, M. P.; Bockrath, M.; Long, J. R.; Park, H. *Nature* **2002**, *417*, 725. (e) Wada, Y. *Ann. N. Y. Acad. Sci.* **2002**, *960*, 39.

(2) Pease, A. R.; Jeppesen, J. O.; Stoddart, J. F.; Luo, Y.; Collier, C. P.; Heath, J. R. *Acc. Chem. Res.* **2001**, *34*, 433.

(3) (a) Tans, S. J.; Verschueren, A. R. M.; Dekker, C. *Nature* **1998**, *393*, 49. (b) Appenzeller, J.; Knoch, J.; Martel, R.; Derycke, V.; Wind, S. J.; Avouris, P. *IEEE Trans. Nanotechnol.* **2002**, *1*, 184. (c) Avouris, P. *Acc. Chem. Res.* **2002**, *35*, 1026.

(4) (a) Lee, J.-O.; Lientschnig, G.; Wiertz, F.; Struijk, M.; Janssen, R. A. J.; Egberink, R.; Reinhoudt, D. N.; Hadley, P.; Dekker, C. *Nano Lett.* **2003**, *3*, 113. (b) Kagan, C. R.; Afzali, A.; Martel, R.; Gignac, L. M.; Solomon, P. M.; Schrott, A. G.; Ek, B. *Nano Lett.* **2003**, *3*, 119.

(5) (a) Singh, R.; Lodha, A. *IEEE Trans. Semicond. Mater.* **2001**, *14*, 281. (b) Saxena, V.; Malhotra, B. D. *Curr. Appl. Phys.* **2003**, *3*, 293. (c) Samuel, I. D. W. *Philos. Trans. R. Soc. London, Ser. A* **2000**, *358*, 193. (d) He, H.; Zhu, J.; Tao, N. J.; Nagahara, L. A.; Amlani, I.; Tsui, R. *J. Am. Chem. Soc.* **2001**, *123*, 7730.

(6) Service, R. F. *Science* **2001**, *293*, 782.

(7) (a) Fendler, J. H. *Chem. Mater.* **2001**, *13*, 3196 and references therein. (b) Tour, J. M. *Acc. Chem. Res.* **2000**, *33*, 791. (c) Carroll, R. L.; Gorman, C. B. *Angew. Chem., Int. Ed.* **2002**, *41*, 4379. (d) Robertson, N.; McGowan, C. A. *Chem. Soc. Rev.* **2003**, *32*, 96. (e) Cahen, D.; Hodes, G. *Adv. Mater.* **2002**, *14*, 789. (f) Allara, D. L.; Dunbar, T. D.; Weiss, P. S.; Bumm, L. A.; Cygan, M. T.; Tour, J. M.; Reinerth, W. A.; Yao, Y.; Kozaki, M.; Jones, L. *Ann. N. Y. Acad. Sci.* **1998**, *852*, 349.

(8) Hipps, K. W. *Science* **2001**, *294*, 536.

(9) (a) Fan, F.-R. F.; Yang, J.; Dirk, S. M.; Price, D. W.; Kosynkin, D. V.; Tour, J. M.; Bard, A. J. *J. Am. Chem. Soc.* **2001**, *123*, 2454. (b) Fan, F.-R. F.; Yang, J.; Cai, L.; Price, D. W.; Dirk, S. M.; Kosynkin, D. V.; Yao, Y.; Rawlett, A. M.; Tour, J. M.; Bard, A. J. *J. Am. Chem. Soc.* **2002**, *124*, 5550. (c) Weiss, P. S.; Bumm, L. A.; Dunbar, T. D.; Burgin, T. P.; Tour, J. M.; Allara, D. L. *Ann. N. Y. Acad. Sci.* **1998**, *852*, 145 and references therein.

(10) (a) Kelley, T. W.; Granstrom, E. L.; Frisbie, C. D. *Adv. Mater.* **1999**, *11*, 261. (b) Gardner, C. E.; Macpherson, J. V. *Anal. Chem.* **2002**, *74*, 576A.

(11) (a) Liau, Y.-H.; Scherer, N. F.; Rhodes, K. *J. Phys. Chem. B* **2001**, *105*, 3282. (b) Planes, J.; Houze, F.; Chretien, P.; Schneegans, O. *Appl. Phys. Lett.* **2001**, *79*, 2993. (c) Gadenne, M.; Schneegans, O.; Houze, F.; Chretien, P.; Desmarest, C.; Sztern, J. Gadenne, P. *Physica B* **2000**, *279*, 94. (d) Macpherson, J. V.; de Mussy, J. P. G.; Delplancke, J. L. *J. Electrochem. Soc.* **2002**, *149*, B306.

(12) (a) Cui, X. D.; Primak, A.; Zarate, X.; Tomfohr, J.; Sankey, O. F.; Moore, A. L.; Moore, T. A.; Gust, D.; G., H.; Lindsay, S. M. *Science* **2001**, *294*, 571. (b) Cui, X. D.; Zarate, X.; Tomfohr, J.; Primak, A.; Moore, A. L.; Moore, T. A.; Gust, D.; Harris, G.; Sankey, O. F.; Lindsay, S. M. *Nanotechnology* **2002**, *13*, 5. (c) Cui, X. D.; Primak, A.; Zarate, X.; Tomfohr, J.; Sankey, O. F.; Moore, A. L.; Moore, T. A.; Gust, D.; Nagahara, L. A.; Lindsay, S. M. *J. Phys. Chem. B* **2002**, *106*, 8609. (d) Leatherman, G.; Durantini, E. N.; Gust, D.; Moore, T. A.; Moore, A. L.; Stone, S.; Zhou, Z.; Rez, P.; Liu, Y. Z.; Lindsay, S. M. *J. Phys. Chem. B* **1999**, *103*, 4006. (e) Rawlett, A. M.; Hopson, T. J.; Nagahara, L. A.; Tsui, R. K.; Ramachandran, G. K.; Lindsay, S. M. *Appl. Phys. Lett.* **2002**, *81*, 3043.

(13) (a) Wold, D. J.; Frisbie, C. D. *J. Am. Chem. Soc.* **2001**, *123*, 5549. (b) Wold, D. J.; Frisbie, C. D. *J. Am. Chem. Soc.* **2000**, *122*, 2970. (c) Wold, D. J.; Haag, R.; Rampi, M. A.; Frisbie, C. D. *J. Phys. Chem. B* **2002**, *106*, 2813. (d) Beebe, J. M.; Engelkes, V. B.; Miller, L. L.; Frisbie, C. D. *J. Am. Chem. Soc.* **2002**, *124*, 11268. (e) Sakaguchi, H.; Hirai, A.; Iwata, F.; Sasaki, A.; Nagamura, T.; Kawata, E.; Nakabayashi, S. *Appl. Phys. Lett.* **2001**, *79*, 3708. (f) Nakamura, T.; Yasuda, S.; Miyamae, T.; Nozoye, H.; Kobayashi, N.; Kondoh, H.; Nakai, I.; Ohta, T.; Yoshimura, D.; Matsumoto, M. *J. Am. Chem. Soc.* **2002**, *124*, 12642.

(14) (a) Dai, H.; Wong, E. W.; Lieber, C. M. *Science* **1996**, *272*, 523. (b) de Pablo, P. J.; Gomez-Navarro, C.; Martinez, M. T.; Benito, A. M.; Maser, W. K.; Colchero, J.; Gomez-Herrero, J.; Baro, A. M. *Appl. Phys. Lett.* **2002**, *80*, 1462. (c) Li, J.; Stevens, R.; Delzeit, L.; Tee Ng, H.; Cassell, A.; Han, J.; Meyyappan, M. *Appl. Phys. Lett.* **2002**, *81*, 910.

(15) (a) Alperson, B.; Cohen, S.; Rubinstein, I.; Hodes, G. *Phys. Rev. B* **1995**, *52*, R17017. (b) Alperson, B.; Rubinstein, I.; Hodes, G. *Phys. Rev. B* **2001**, *63*, 081303.

(16) Loiacono, M. J.; Granstrom, E. L.; Frisbie, C. D. *J. Phys. Chem. B* **1998**, *102*, 1679.

(17) (a) Skotheim, T. A.; Elsenbaumer, R. L.; Reynolds, J. R. *Handbook of Conducting Polymers*; Marcel Dekker: New York, 1997; Vols. 1−2. (b) Nalwa, H. S. *Handbook of Organic Conductive Molecules and Polymers*; Wiley: Chichester, UK, 1997; Vols. 1−4. (c) Park, S.-M. In *Handbook of Organic Conductive Molecules and Polymers*; Wiley: Chichester, UK, 1997; Vol. 3.

(18) (a) Yang, R.; Smyrl, W. H.; Evans, D. F.; Hendrickson, W. A. *J. Phys. Chem* **1992**, *96*, 1428. (b) Jeon, D.; Kim, J.; Gallagher, M. C.; Willis, R. F. *Science* **1992**, *256*, 1662. (c) Ho, P. K.; Zhang, P.-C.; Zhou, L.; Li, S. F. Y.; Chan, H. S. O. *Phys. Rev. B* **1997**, *56*, 15919. (d) Bonnell, D. A.; Angelopoulos, M. *Synth. Met.* **1989**, *33*, 301. (e) Cornelison, D. M.; Bowman, G. E.; Porter, T. L.; Caple, G. *Synth. Met.* **1993**, *58*, 383. (f) Ouyang, M.; Huang, J.-L.; Lieber, C. M. *Annu. Rev. Phys. Chem.* **2002**, *53*, 201. (g) Tromp, R. M. *J. Phys.: Condens. Matter* **1989**, *1*, 10211.

(19) (a) Semenikhin, O. A.; Jiang, L.; Iyoda, T.; Hashimoto, K.; Fujishima, A. *J. Phys. Chem.* **1996**, *100*, 18603. (b) Semenikhin, O. A.; Jiang, L.; Iyoda, T.; Hashimoto, K.; Fujishima, A. *Electrochim. Acta* **1997**, *42*, 3321. (c) Barisci, J. N.; Stella, R.; Spinks, G. M.; Wallace, G. G. *Electrochim. Acta* **2000**, *46*, 519.

(20) Ko, J. M.; Rhee, H. W.; Park, S.-M.; Kim, C. Y. *J. Electrochem. Soc.* **1990**, *137*, 905.

(21) Penner, R. M.; Van Dyke, L. S.; Martin, C. R. *J. Phys. Chem.* **1988**, *92*, 5274.

(22) Visit, for example, http://www.molec.com.

(23) (a) Sadki, S.; Schottland, P.; Brodie, N.; Sabouraud, G. *Chem. Soc. Rev.* **2000**, *29*, 283. (b) Suarez, M. F.; Compton, R. G. *J. Electroanal. Chem.* **1999**, *462*, 211. (c) Hwang, B. J.; Santhanam, R.; Lin, Y.-L. *J. Electrochem. Soc.* **2000**, *147*, 2252.

(24) Park, D.-S.; Shim, Y.-B.; Park, S.-M. *J. Electrochem. Soc.* **1993**, *140*, 609.

(25) Warren, L. F.; Anderson, D. P. *J. Electrochem. Soc.* **1987**, *134*, 101.

(26) Kupila, E. L.; Kankare, J. *Synth. Met.* **1996**, *82*, 89.
(27) Ouyang, J.; Li, Y.-F. *Polymer* **1997**, *38*, 1971.
(28) Zhou, M.; Heinze, J. *J. Phys. Chem. B* **1999**, *103*, 8451.
(29) See, for example, Park, W. I.; Yi, G.-C.; Kim, J.-W.; Park, S.-M. *Appl. Phys. Lett.* **2003**, *82*, 4358, in which exactly the same equipment as used in this study had been used.
(30) (a) Hoier, S. N.; Park, S.-M. *J. Phys. Chem.* **1992**, *96*, 5188. (b) Lee, H. J.; Cui, S.-Y.; Park, S.-M. *J. Electrochem. Soc.* **2001**, *148*, D139. (c) Bredas, J. L.; Themans, B.; Fripiat, J. G.; Andre, J. M. *Phys. Rev. B* **1984**, *29*, 6761.
(31) (a) Vassiliev, S. Y.; Jackowska, K.; Frydrychevicz, A.; Tsirlina, G. A.; Petrii, O. A. *Electrochim. Acta* **2001**, *46*, 4043. (b) Joo, J.; Long, S. M.; Pouget, J. P.; Oh, E. J.; Macdiarmid, A. G.; Epstein, A. J. *Phys. Rev. B* **1998**, *57*, 9567. (c) Zuo, F.; Angelopoulos, M.; Macdiarmid, A. G.; Epstein, A. J. *Phys. Rev. B* **1987**, *36*, 3475. (d) Li, Q.; Cruz, L.; Phillips, P. *Phys. Rev. B* **1993**, *47*, 1840.